Journal of Cleaner Production 188 (2018) 911–920

Contents lists available at ScienceDirect

Journal of Cleaner Production

journal homepage: www.elsevier.com/locate/jclepro

Bi-objective optimization of biochar-based carbon management networks

Beatriz A. Belmonte [a, b], Michael Francis D. Benjamin [b, c], Raymond R. Tan [a, *]

[a] Chemical Engineering Department, De La Salle University, 2401 Taft Avenue, 0922, Manila, Philippines
[b] Chemical Engineering Department, University of Santo Tomas, España Blvd, 1015, Manila, Philippines
[c] Research Center for the Natural and Applied Sciences, University of Santo Tomas, España Blvd, 1015, Manila, Philippines

ARTICLE INFO

Article history:
Received 22 December 2017
Received in revised form
31 March 2018
Accepted 3 April 2018
Available online 4 April 2018

Keywords:
Biochar
Negative emissions technology
Bi-objective optimization
Carbon management network
Source-sink model
Mixed-integer linear programming

ABSTRACT

Biochar is the carbon-rich solid product derived from thermochemical processing of biomass. Its application to soil can sequester atmospheric carbon, leading to negative net emissions, while also improving agricultural yield. Biochar-based carbon management networks thus have the potential for scalable contributions to climate change mitigation efforts. However, it is necessary to allocate biochar of suitable quality to appropriate sinks, based on contaminant tolerance limits of soil. In this work, the network is modelled as a bi-objective mixed integer linear programming model, with profit and carbon sequestration as the objective functions. The model calculates the optimum allocation of biochar such that their prescribed limits for the contaminants are met. A Philippine case study is solved under different scenarios to illustrate the practical use of the developed model. The results provide useful insights for the rational decision-maker to arrive at the most preferred solution among the Pareto optimal choices. Comparison of the two scenarios substantiate the significance of unique sequestration factor as an additional parameter in the model to account for the interactions between the soils and biochars so that the maximum sustainable potential of biochar in climate change mitigation can be properly assessed.

1. Introduction

Atmospheric carbon dioxide concentration recently reached 410 ppm this year, the highest level in recorded history (Kahn, 2017). Thus, there is now an urgent need to balance economic growth targets, especially in developing countries, with CO_2 emissions constraints (Lee et al., 2017). To stabilize global climate, carbon sequestration as one of the potential levers for mitigating climate change; should be deployed at large scales in the near future (Xu and Ramanathan, 2017). One of the available options is biochar, the carbon-rich solid co-product from the gasification or pyrolysis of biomass. Biochar can be applied to soil in the same manner as compost from agricultural waste as a climate change mitigation strategy (Bong et al., 2017). Biochar application is a negative emission technology (NET) that is estimated to be capable of mitigating 130 Gt of carbon until 2100 via direct sequestration in biochar coupled with beneficial secondary effects (Woolf et al., 2010). These secondary effects result from the displacement of fossil fuels by energy co-products from biochar production, the suppression of soil N_2O and CH_4 fluxes when biochar is added to soil, the displacement of fossil fuel-intensive synthetic fertilizers due to improved soil fertility, and the reduction of energy requirement for irrigation due to improved water retention properties.

Biochar can be produced from various biomass feedstocks through gasification or pyrolysis. These pathways yield biochar along with different proportions of co-products in gaseous (syngas) or liquid (bio-oil) form (Vereš et al., 2014). The carbon in biochar is mostly recalcitrant (i.e., inert) so that it becomes permanently sequestered over multiple centuries when added to soil. A relatively small percentage of the carbon is labile (i.e., reactive) and thus decomposes rapidly to be released into the natural carbon cycle. In this regard, biochar application to soil is gaining considerable interest as a carbon management strategy (Muñoz et al., 2017). Because of the aforementioned secondary effects on greenhouse gas (GHG) emissions, the total potential for mitigation can be much larger than the physical carbon content of the biochar. Such optimal benefits can result from proper matching of biochar with

* Corresponding author.
E-mail address: raymond.tan@dlsu.edu.ph (R.R. Tan).

https://doi.org/10.1016/j.jclepro.2018.04.023
0959-6526/

receiving soils that act as carbon sinks. A consistently reported mechanism for improved crop yield is liming effect due to increase in soil pH (Tan et al., 2017). Various feedstocks that offer financial viability are residual biomass such as forest or wood by-products and agricultural residues that include bagasse from sugarcane, corn stover, rice husks, cereal straw, and coconut shells (Jirka and Tomlinson, 2014). Thus, biochar production can also be considered as a potential strategy to address waste management challenges. Windeatt et al. (2014) estimated the carbon sequestration potential of biochar produced from agricultural waste (i.e., coconut husk, coconut shell, olive pomace, palm kernel shell, rice husk, cotton stalk, sugarcane bagasse and wheat straw) at current global availability to be 5.5×10^8 t/y of CO_2. Biochar is a relatively simple and mature technology process that can be deployed easily even in developing nations (McGlashan et al., 2012). Commercial-scale biochar-based carbon management networks (CMNs) can be economically viable through simultaneous generation of valuable co-products (Wrobel-Tobiszewska et al., 2015) and carbon trading scheme (Galinato et al., 2011).

The climate change mitigation potential of biochar depends on feedstock, processing conditions, types of soil and the corresponding environmental conditions. The variability in recalcitrance and carbon content of biochar from different feedstocks results in different levels of efficacy for carbon sequestration (Windeatt et al., 2014). Increasing the pyrolysis temperature increases the release of volatiles, giving a higher level of recalcitrant carbon in the product (Crombie et al., 2013). However, increasing the gas phase flow rate decreases the yield and recalcitrant carbon content of biochar (Crombie and Mašek, 2015). Secondary effects are particularly sensitive to the properties of both the biochar and the receiving soil. For example, acidic soils release more CO_2 compared to neutral and alkaline soils upon biochar addition (Sheng et al., 2016). On the other hand, CO_2 fluxes revealed positive response to biochar amendment in soils with coarse and medium texture (He et al., 2017). Proper evaluation of these factors is important to have a more acceptable estimation of the carbon sequestration potential of biochar. Such allocation decisions can be facilitated with the aid of rigorous models.

Biochar represents an emerging technology and is yet to be proven scalable and cost-effective alternative to mitigate climate change. McLaren (2012) rated biochar as being intermediate (i.e., 4–6 in a scale of 1–9) in terms of technology readiness level (TRL). This implies that there is a need for further research to deploy biochar-based CMNs and optimize the climate change mitigation benefits. Barriers to large-scale use of biochar as a carbon management strategy include the risk of adverse environmental impacts from its contaminants, as well as techno-economic challenges due to the market for higher-value alternative uses. Process Systems Engineering (PSE) can provide tools and models to aid in the planning of large-scale biochar-based CMNs (Belmonte et al., 2017). Quantitative approaches can guide the proper deployment of biochar-based systems in order to scale up the benefits while minimizing the potential for adverse environmental effects. The optimal synthesis of biochar-based CMNs was first addressed by Tan (2016). A mixed integer linear programming model (MILP) was developed to find the optimum allocation of biochar with varying contaminant levels to different soils acting as biochar sinks, with prescribed storage capacities and quality requirements over multiple time periods.

The model proposed by Tan (2016) relies on a source-sink formulation extensively used in various Process Integration (PI) problems. However, it relies on simplifications that limit its applicability. This work develops an improved version of the model by accounting for more relevant and practical details. The first improvement is the use of a second objective function (i.e., profit) in addition to carbon sequestration. The second improvement accounts for the dependence of total carbon sequestration on source-sink interactions. A unique *sequestration factor* for each source-sink pair is proposed in view of the recent findings from biochar literature that the carbon sequestration potential of biochar does not only depend on the processing conditions or choice of feedstock, but also on the type and quality of the soil in which the biochar is applied. The rest of this paper is organized as follows. In the next section, an illustration of the overall methodology is presented. A description of the formal problem statement follows. Afterwards, the mathematical formulation and model limitations are given. The enhanced model is applied to a semi-hypothetical case study using a specific geographical region in the Philippines to demonstrate a plausible scenario of the commercial-scale biochar-based CMN. Future works and conclusions are then given in the final part of this paper.

2. Methodology for the planning of biochar-based CMN

Fig. 1 represents the process to optimize the biochar supply network. The first step is data collection via extensive literature review on which to base the plausible values for the model parameters and to define the planning problem. To address the planning problem, quantitative model is then developed with the aid of mathematical programming. Then the model is tested and validated via sensitivity analysis and illustrative case study which consider different scenarios yielding the optimal solutions. The generated optimal solutions are further analyzed to find sound decision options that will guide the decision-makers to select the most preferred solution.

2.1. Formal problem statement

The planning problem, whose superstructure representation is given in Fig. 2, can be stated formally as follows:

- The biochar-based CMN is comprised of a set of pyrolysis plants selected as sources $i \in I$ $(i = 1, 2, 3 \ldots M)$ producing biochars that are to be allocated to a set of croplands chosen as sinks $j \in J$ $(j = 1, 2, 3 \ldots N)$ throughout a specified period, divided into time intervals $p \in P$ (periods, $p = 1, 2, 3 \ldots T$).
- The limits of each flowrate and levels of undesirable impurities coming from source i $k \in K$ (contaminants, $k = 1, 2, 3 \ldots Q$) are prescribed.
- Every sink j can only receive biochar up to a defined maximum flowrate, maximum storage capacity and maximum tolerance level for each impurity k.
- For each potential source-sink pair, the carbon footprint (i.e., from the handling, transportation and application) as well as the sequestration factor (i.e., direct and indirect benefits) per unit of biochar are known.
- The problem is to determine how to allocate biochar from each source i to each sink j in each time interval p to maximize both CO_2 sequestration and profitability.

2.2. Mathematical model formulation

The MILP model developed by Tan (2016) for planning biochar-based CMNs is extended and modified here. The relevant modifications are given by Eq. (1)–(2). The original MILP formulations are shown in the Appendix. The reader is likewise referred to the work of Tan (2016) for a more detailed discussion. The problem is concerned with mathematical optimization involving two objective functions to be optimized simultaneously. One of the objective functions is to maximize the net CO_2 sequestration of the system

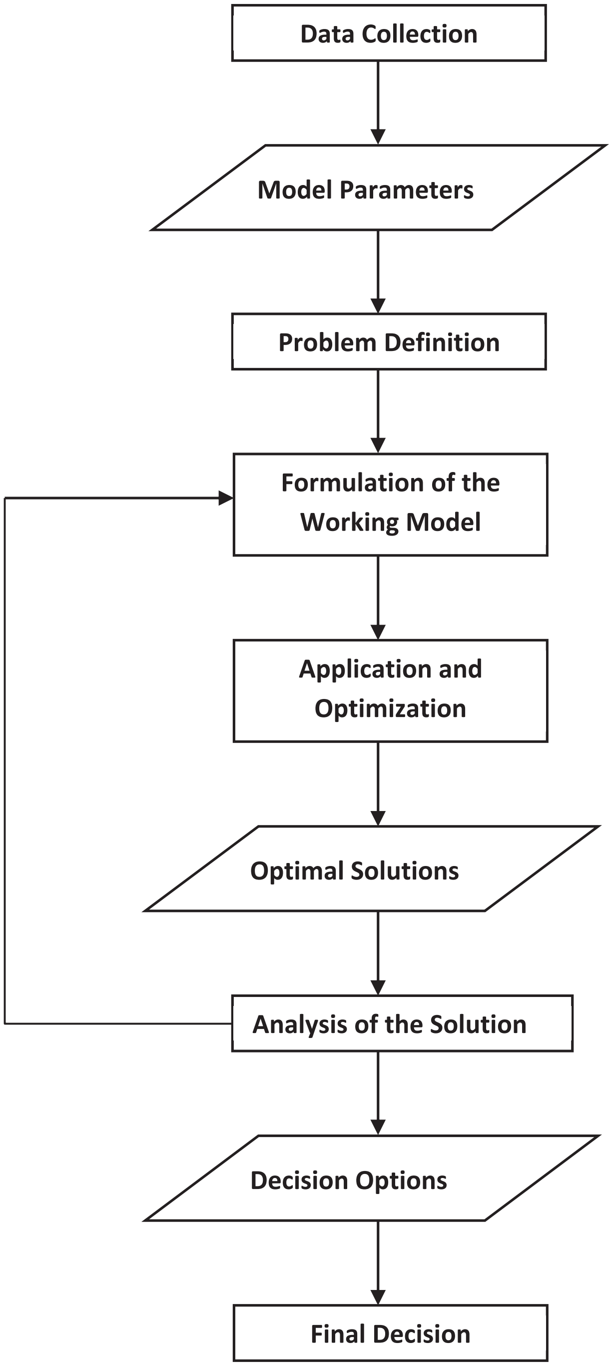

Fig. 1. Flowchart representing the methodology for the planning of biochar-based CMN.

throughout the period specified by the model:

$$\max\ \Sigma_i\Sigma_j\Sigma_p A_{ij}x_{ijp} - \Sigma_i\Sigma_j\Sigma_p B_{ij}x_{ijp} \tag{1}$$

The parameter A_{ij} (t CO_2/t) is the sequestration factor of biochar from source i to sink j which provides the amount of CO_2 sequestered for each unit mass of biochar. A unique sequestration factor is assigned per source-sink pair to consider the impact of the sink in assessing the full potential of biochar in climate change mitigation. This is the most important feature introduced in this improved model. The CO_2 emissions from transporting, handling and applying the biochar are denoted by B_{ij} (t CO_2/t). The variable x_{ijp} (t/y) is the quantity of biochar coming from source i which is to be applied to sink j in period p.

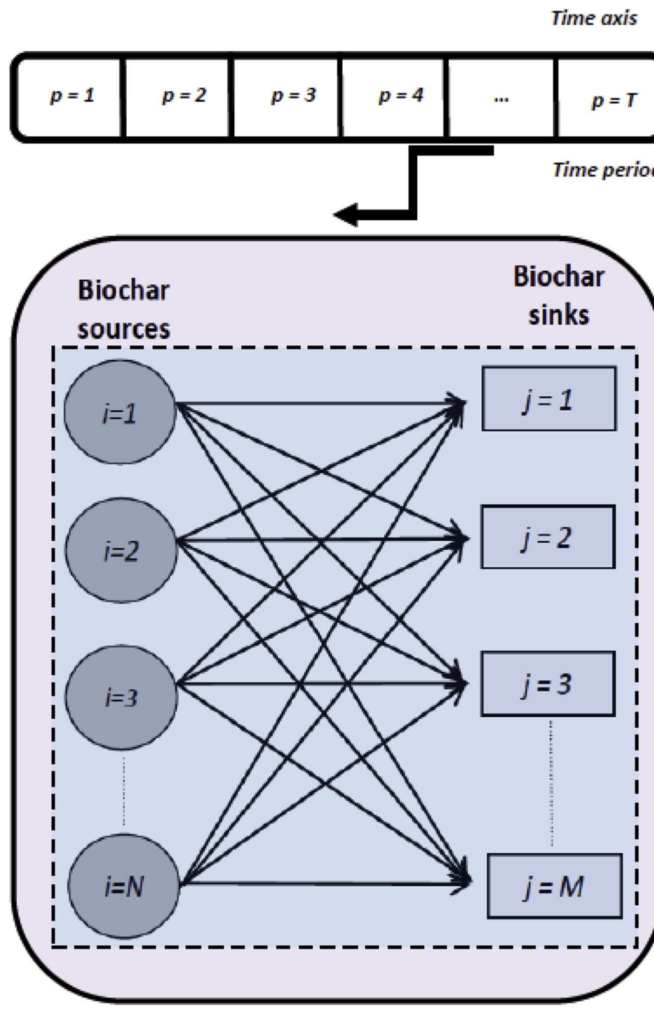

Fig. 2. Source-sink superstructure for biochar network.

The second objective function is to maximize annual profitability during the planning horizon and is given by:

$$\max\ \left(\Sigma_i\Sigma_j\Sigma_p BCx_{ijp} + \Sigma_i\Sigma_j\Sigma_p Cf_i x_{ijp}BO\right) - \left(\Sigma_i\Sigma_j\Sigma_p PCx_{ijp} + \Sigma_i\Sigma_j\Sigma_p \frac{x_{ijp}}{Vc} \times 2d_{ij}Cv + \Sigma_i\Sigma_j\Sigma_p ACx_{ijp}\right) \tag{2}$$

where coefficients BC and BO denote biochar and bio-oil unit price in US$/t respectively while parameter Cf_i is the dimensionless conversion factor of bio-oil from source i derived from the experimental analysis of Windeatt et al. (2014). The amount of bio-oil is a function of x_{ijp} and Cf_i. The cost of biochar production per unit mass is represented by PC (US$/t). The capacity of vehicles needed to deliver the biochar to the sink is denoted by Vc (t/vehicle). The distance from biochar source i down to its final destination j is given by d_{ij} (km). This distance must be doubled to denote vehicle round trip. The cost of transportation is designated by Cv (US$/km), while the application cost for each unit mass of biochar is given by AC (US$/t). Profit maximization is incorporated in the model since biochar-based CMN that considers both economic and environmental performances can sufficiently guide decision-makers in satisfying their subjective preferences. The illustrative case study

clearly demonstrates the applicability of the extended model.

2.3. Model limitations

The science of biochar production and application has indeed made rapid progress in the past decade. However, there are still relevant aspects of biochar research wherein the existing level of knowledge is limited. The following aspects are beyond the scope of the current model, but need to be addressed eventually:

- Risks and uncertainties resulting from potential soil contaminants can further be managed when experimental data and long-term field investigation reports are available as these inputs can further be included in the model (i.e., mechanism behind leaching of soil contaminants). Another effective strategy to overcome or minimize deleterious environmental effect is through customization of biochar properties to potentially manage specific soil. This is an interesting feature that can be incorporated in the model.
- The transportation of various biomasses to the locations of biochar pyrolysis plants would entail additional cost and indirect carbon emissions, hence, will affect the values of the objective functions. This aspect can be accounted for separately or appropriate model parameters can be redefined in the future. Also, additional constraints and equations can be incorporated in the model to extend the system boundary from the transportation of biomass from different sources to the application of biochar to agricultural lands. The network can also include processes relating to the production and collection of biomass (e.g., grinding, chipping, pelletization) before its destination to the pyrolysis plants.
- Decision-makers can have the inclination to prioritize profit over carbon sequestration or vice versa. On the other hand, they could also choose to balance profit and environmental impact. Selection of the most preferred solution from the set of Pareto-optimal solutions can be done by different techniques. For instance, the most preferred solution can be selected by employing the analytical hierarchy process (AHP) to set the weights (importance with respect to the others as input by the decision-maker) of the different criteria (objectives) and multiply the normalized values of the objectives of each solution with the corresponding weights assigned to generate the score of each solution. The score will influence the final decision. On the other hand, other approach such as Fuzzy based membership function method can also be used to determine the best compromised solution.
- The model's solution is clearly dependent on the values of the key parameters such as sequestration factors and biochar price. Currently, there is very limited knowledge on the mechanism behind biochar-soil interactions and their effects on the carbon sequestration capability of biochar. Moreover, biochar prices depend very much on the origin of production sites (Ahmed et al., 2016). To handle these uncertainties, it is interesting to study the variations in the different key parameters and their impact to the final results. This aspect can be addressed via fuzzy MILP, Monte Carlo, etc.
- Sensitivity analysis of transportation distance can be conducted to determine the extent to which the biochar system will remain profitable based on realistic study assumptions (as this could further determine the appropriate mode of transport).

2.4. Illustrative case study

A case study is given here that represents Central Luzon region in the Philippines (Fig. 3), which is one of the leading regions that produce agricultural crops and residual biomass resources in the country. It has a total land area of 2,190,619 ha (approximately 7% of the total area of the Philippines), wherein 552,104 ha are agricultural lands ("Regional Profile: Central Luzon," n.d.). These highly productive lands make them ideal locations for pyrolysis plants that can utilize coconut shell, rice husk, and sugarcane bagasse as feedstocks. The combined maximum annual production of coconut, rice, and sugarcane is 2,397,608 t/y, which can potentially generate 1,012,947 t/y of agricultural waste (i.e., coconut shell, rice husk, and sugarcane bagasse). This in turn is approximately equivalent to

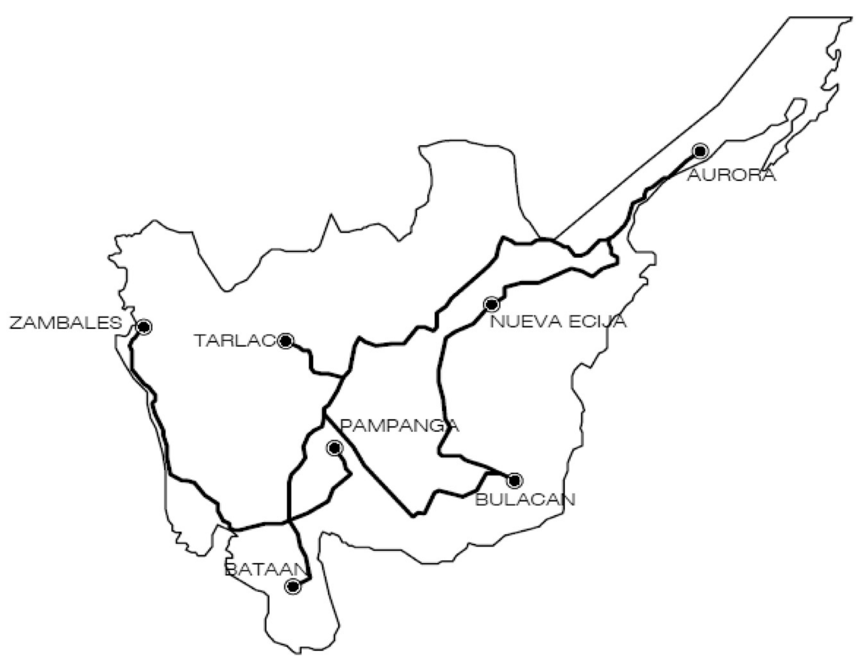

Fig. 3. Location of biochar sources and sinks.

346,459 t/y of biochar that can directly sequester around 848,183 t/y of CO_2 (assuming that there is no limit in soil storage capacity). It is perceived here that a potentially more valuable market for biochar as a soil amendment agent is for high value crops such as fruits. Organic farmers can consider biochar as a desirable soil additive for their crops. Hence, farms growing such crops are chosen as potential sinks for biochar.

Three metals (Na, Mg and Ca) in biochar are considered in the case study. These elements can form salts which can negatively affect the agricultural productivity for many crops when they reach an excess concentration in soil, and can thus hinder the optimum plant growth or yield (Abdul Qados, 2011). Table 1 presents the data for the three sources chosen in the case study that supply different types of biochar produced from various biomass residues namely sugarcane bagasse, rice husk and coconut shell respectively. The range of production rate and the sequestration factor of each source are indicated. The metal content in biochar used in the case study is a function of biomass feedstock and is based from the paper of Tan et al. (2017). The case study also uses a ten-year operation time framework. The operation of Sources 1 and 2 is throughout this period while Source 3 starts only its operation in the third year. The characteristics of the four sinks are depicted in Table 2 in which different crops are grown such as banana, pineapple, coffee and mango. The cropland area of each sink is based on the average area harvested for coffee and fruit crops such as banana, pineapple and mango per province. Crop production data for the years 2007–2016, from the Philippine Statistics Authority's (PSA) statistical database; CountrySTATPhilippines, was used to determine the average area harvested or planted ("Regional Profile: Central Luzon," n.d.). The storage capacity is computed based on the application dosage recommended from published literature ranging from 5 to 50 t/ha (Major, 2010). The storage capacity is equally split within a ten-year planning horizon to get the annual application rate limit. The last three columns of Table 2 provide the assumed maximum levels of metal contents in biochar that can be applied without rendering any harm to the receiving soil. In practice, salinity tolerance is a result of different attributes which depend on physiological interactions that cannot be easily determined (Abdul Qados, 2011). The distances between the biochar sources and sinks are given in Table 3. The carbon emission footprint of transporting biochar by truck is 0.1 kg CO_2/t/km (Foo et al., 2013). Table 4 gives the data used for cost calculations in the case study. To date, a major industrial biochar market does not exist from which to base biochar price and cost data for a more accurate estimation (Ahmed et al., 2016). The cost of equipment mainly represents the production cost. In the Philippines, the biochar production cost is estimated as US$100.50/t (Fornes et al., 2015). The capacity of the vehicle which is to be used for transporting the biochar is 25 t. The cost of transportation is given as US$1.535/km. It is assumed that the unit cost of biochar application to soil is US$6.58/t (Kulyk, 2012). The market price of bio-oil in the case study is US$103/t (Kasivisvanathan et al., 2012). Given the high variability of biochar prices, its market price in the Philippines is assumed to be US$50/t which is within the range of biochar market price so that a farmer can potentially earn profit when a carbon offset market exists (Galinato et al., 2011). Table 5 shows the dimensionless conversion factor of bio-oil from each source derived from the experimental analysis of Windeatt et al. (2014). Two

Table 1
Biochar source data for the case study.

Source	Minimum production rate, S_{ip}^{L} (t/y)	Maximum production rate, S_{ip}^{U} (t/y)	Sequestration factor, A_{ij} (t CO_2/t)	Biochar Na content, Q_{i1p} (g/t)	Biochar Mg content, Q_{i2p} (g/t)	Biochar Ca content, Q_{i3p} (g/t)	Years of operation
Aurora (Coconut shell, $i = 1$)	6000	8000	3.43	80	150	4600	1–10
Nueva Ecija (Rice husk, $i = 2$)	20,000	26,000	2.00	2900	10,400	5000	1–10
Tarlac (Bagasse, $i = 3$)	10,000	13,000	3.25	300	1300	2600	3–10

Table 2
Biochar sink data for the case study.

Sink	Area (ha)	Application dosage (t/ha)	Storage capacity, L_j (t)	Limiting biochar flowrate, D_{jp} (t/y)	Limiting biochar Na content, Q_{j1}^{*} (g/t)	Limiting biochar Mg content, Q_{j2}^{*} (g/t)	Limiting biochar Ca content, Q_{j3}^{*} (g/t)
Pampanga ($j = 1$)	1922	35	67,270	6727	750	2600	1250
Bataan ($j = 2$)	1692	50	84,600	8460	7250	26,000	12,500
Bulacan ($j = 3$)	10,750	20	215,000	21,500	1500	5200	2500
Zambales ($j = 4$)	9483	10	94,830	9483	2900	10,400	5000

Table 3
Transportation distances in km for source-sink pairs in the case study.

Source	Distance, d_{ij} (km)			
	Sink			
	Pampanga $j = 1$	Bataan $j = 2$	Bulacan $j = 3$	Zambales $j = 4$
Aurora (Coconut shell, $i = 1$)	257	303	238	232
Nueva Ecija (Rice husk, $i = 2$)	93.5	173	99	265
Tarlac (Bagasse, $i = 3$)	65.2	123	122	210

Table 4
Cost data for the case study.

Parameter	Values	Reference
Production cost (*PC*)	US$ 100.50/t	(Fornes et al., 2015)
Capacity of vehicle (*Vc*)	25 t	
Specific vehicle transport cost (*Cv*)	US$ 1.535/km	
Biochar application cost (*AC*)	US$ 6.58/t	(Kulyk, 2012)
Biochar price(*BC*)	US$ 50/t	(Galinato et al., 2011)
Bio-oil price (*BO*)	US$ 103/t	(Kasivisvanathan et al., 2012)

Table 5
Dimensionless conversion factor of bio-oil from each source.

Source	Cf_i	Reference
Aurora (Coconut shell $i = 1$)	1.55	(Windeatt et al., 2014)
Nueva Ecija (Rice husk, $i = 2$)	0.86	(Windeatt et al., 2014)
Tarlac (Bagasse, $i = 3$)	1.82	(Windeatt et al., 2014)

scenarios are presented. The first scenario focuses on the use of sequestration factor that depends only on the type of biomass feedstock while the second one employs a unique sequestration factor per source-sink pair. The MILP model described above was employed using the commercial optimization software LINGO 17.0 and solved with negligible CPU time using a laptop with 8.00 GB RAM, i7-7500UCPU and a 64-bit operating system running on Windows 10 Home Single Language.

3. Results and discussion

3.1. Scenario 1 - sequestration factor depends only on the type of biomass feedstock

In this scenario, the sequestration factor is calculated based only on the characteristics of raw feedstock and the resulting biochar product as analyzed by Windeatt et al. (2014). The corresponding sequestration factor of biochars from each type of residual biomass feedstock used in the case study is presented in Table 1. The bi-objective optimization is performed via the ε-constraint method (Haimes and Hall, 1974). A brief discussion of the method is given in the Appendix. The trade-off between CO_2 sequestration and profitability is depicted in Fig. 4 for the different values of ψ. The risk aversion parameter ψ (see Equation (A.5) in the Appendix) is incorporated in the model to account for the uncertainty arising on the difficulty of finding the level of impurity that can be tolerated by the receiving soil. This parameter quantifies the willingness of the decision-maker to allow contamination in the soil. If the decision-maker wants to completely avoid the risk in applying

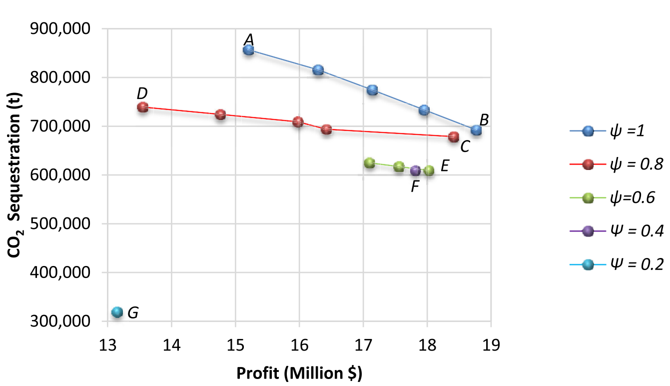

Fig. 4. Comparison of Pareto-optimal sets for each value of ψ (Scenario 1).

biochar to soil, its value is zero. On the other hand, its value is unity for a decision-maker who is not averse to let soil contaminant levels reach the prescribed limit. The MILP model is solved for $\psi = 1$, 0.8, 0.6, 0.4 and 0.2. It is clear that each point of each Pareto front can be taken as a solution to the problem depending on the decision-maker. It can be seen that as ψ decreases, the points in each Pareto front that correspond to the solutions generated approach each other indicating the possible existence of a unique solution for lower values of the parameter ψ. For $\psi = 0.4$ and 0.2, there exists a single solution that simultaneously optimizes both objectives denoted by points *F* and *G* in Fig. 4. For instance, the net CO_2 sequestration achieved by the system during the 10-year period of operation are 609,181.7 t and 319,206.4 t for $\psi = 0.4$ and 0.2 respectively. The corresponding optimum profit for $\psi = 0.4$ and 0.2 are US$17,813,080 and US$13,145,450 respectively.

Each point in each Pareto front corresponds to a particular biochar source-sink network. At $\psi = 1$, the selected network represented by point *A* (see Fig. 4) with a net CO_2 sequestration of 856,748 t and a profit of US$15,200,340 is given in Table 6. The first value in each cell gives the amount of biochar allocated for each sink from the first two operational years. The next number denotes the biochar allocation during the last eight years. When Source 3 becomes operational, the allocation from the third to the tenth years in Sinks 1 and 3 of Table 6 changes. The model recommends blending of biochar at Sink 3 during the ten-year time frame so as not to exceed the limit prescribed for each contaminant. For instance, blending of 8000 t/y of biochar coming from Source 1 (contains 80 g Na/t, 150 g Mg/t and 4600 g Ca/t) with 3390 t/y of biochar coming from Source 2 (contains 2900 g Na/t, 10,400 g Mg/t and 5000 g Ca/t) produces 11,390 t/y of biochar that contains 919.315 g Na, 3200.702 g Mg and 4719.052 g Ca per t of biochar during the first two years of operation at Sink 3. The net carbon sequestration for the first two years is 72,832.257 t/y which is the difference between 73,469.6 t/y of CO_2 directly sequestered in biochar and 637.343 t/y of CO_2 emitted from transportation. On the other hand, the net carbon sequestration for the remaining eight years of operation is 88,885.561 t/y which is the difference between 89,479.6 t/y of direct CO_2 sequestration in biochar and 594.039 t/y of emissions from transportation. Therefore, during the 10 operational years the total cumulative CO_2 sequestration attained by the biochar-based network is 856,748 t which is equal to the difference of 862,776 t (73,469.6 t/y x 2y + 89,479.6 t/y x 8y) and 6026.998 t (637.343 t/y x 2y + 594.039 t/y x 8y). The projected income from the sale of biochar is US$17,747,380 while the expected revenue from bio-oil amounts to US$42,861,890. The costs of biochar production, transportation and application to soil are US$35,672,220, US$7,401,143 and US$2,335,555 respectively. Thus, the total system profit during the 10-year period of operation is US$15,200,340.

As can be seen in Fig. 4, a trade-off also exists between CO_2 sequestration and soil contamination risk. For a decision maker who is not willing to risk soil contamination higher than 80% of the prescribed physical limit but eager to earn the highest possible profit, a solution denoted by point *C* is the best option. It is interesting to note that the solution represented by point *C* is only 1.99%

Table 6
Biochar source-sink network for $\psi = 1$, net CO_2 sequestration = 856,748 t, profit = US$ 15,200,340: Scenario 1 (biochar flowrates in t/y).

Source	Sink				
	1	2	3	4	Total
1			8000; 0		8000; 0
2	1681.8; 0	8460; 8460	3390; 5671.8	9483; 9483	23,014.8; 23,614.8
3	0; 3234.1		0; 9765.9		0; 13,000
Total	1681.8; 3234.1	8460; 8460	11,390; 15,438	9483; 9483	

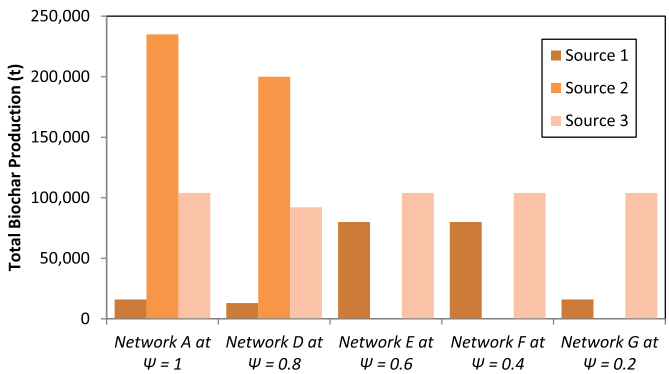

Fig. 5. Total biochar production by source for selected networks at different values of ψ within the ten-year planning horizon in Scenario 1.

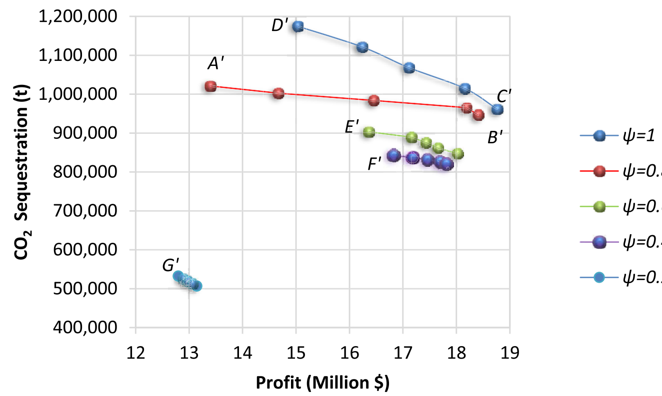

Fig. 6. Comparison of Pareto-optimal sets for each value of ψ (Scenario 2).

lower in CO_2 sequestration potential and 1.9% lower in profit compared to the solution denoted by point *B*.

Selected networks corresponding to solutions denoted by points *D*, *E*, *F* and *G* (see Fig. 4) are given in the Supplementary Material, Tables S1-S4. A decrease in biochar production from Source 2 occurs when ψ is set at a value of 0.8 and the supply of biochar from Source 2 is entirely eliminated at $\psi = 0.6$, 0.4 and 0.2 (Fig. 5). This result is notable since Source 2 produces biochar that contains the highest level of metal contaminants.

3.2. Scenario 2 - unique sequestration factor per source-sink pair

The sequestration factor is varied per source-sink pair to provide a higher accuracy assessment of the potential of biochar to mitigate climate change within the biochar-based CMN. In this scenario a unique sequestration factor is assigned to each source-sink pair (see Table 7) to signify that the total emissions abatement of biochar does not only depend on feedstock and processing conditions but also on other factors such as the type of cropland to which biochar is applied and the corresponding environmental conditions.

The MILP model is implemented and the resulting Pareto optimal choices are plotted in Fig. 6 for the different values of ψ. It is evident that the points in each Pareto front draw nearer as the value of ψ decreases. This minimizes the difficulty of arriving at an appropriate decision since the values of the objective functions are

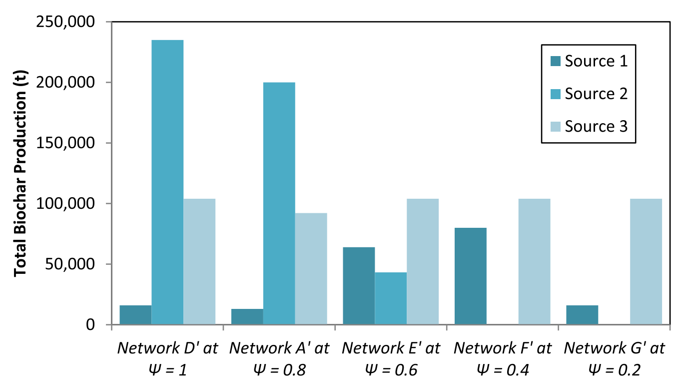

Fig. 7. Total biochar production by source for selected networks at different values of ψ within the ten-year planning horizon in Scenario 2.

getting closer as ψ decreases. The Pareto front corresponding to $\psi = 0.8$ is notable in the way that the solution denoted by point *B*′ is only 7.29% lower in CO_2 sequestration but 37.4% higher in profitability relative to the solution represented by point *A*'. In addition, compared to solution *C*′, the values of the CO_2 sequestration and profitability of solution *B*' are only 1.55% and 1.9% lower respectively and the soil contamination risk is reduced by 20%. Meanwhile, a significant decrease in CO_2 sequestration and profitability is observed at $\psi = 0.2$.

Table 7
Unique sequestration factor per source-sink pair used in the case study (Scenario 2).

Source	Unique sequestration factor, A_{ij}			
	Sink			
	Pampanga $j = 1$	Bataan $j = 2$	Bulacan $j = 3$	Zambales $j = 4$
Aurora (Coconut shell, $i = 1$)	3.86	4.29	4.72	5.15
Nueva Ecija (Rice husk, $i = 2$)	2.25	2.50	2.75	3.00
Tarlac (Bagasse, $i = 3$)	3.66	4.06	4.47	4.88

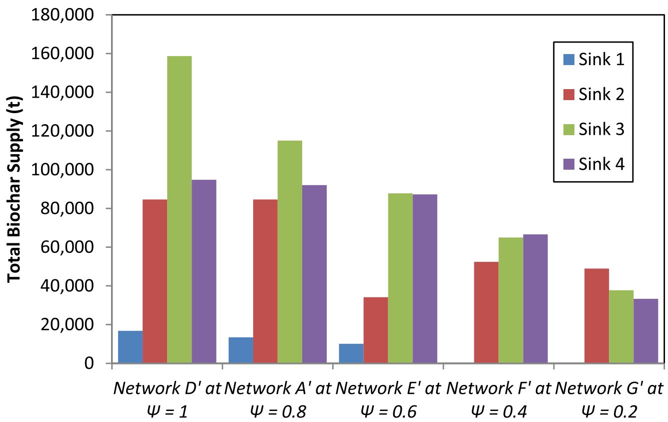

Fig. 8. Total biochar supply to each sink for selected networks at different values of ψ within the ten-year planning horizon in Scenario 2.

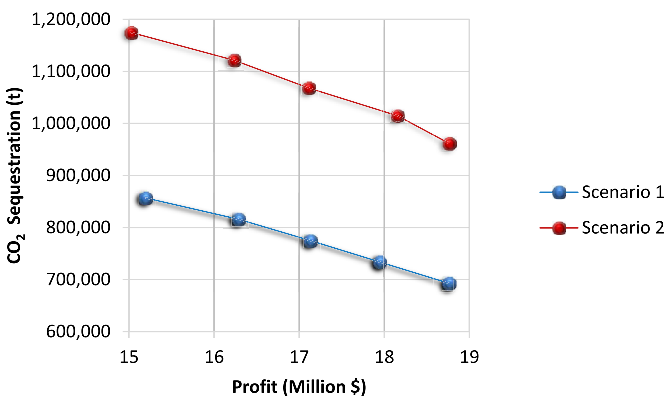

Fig. 9. Comparison of pareto frontiers of Scenarios 1 and 2 at $\psi = 1$.

Representative networks as designated by points D', A', E', F' and G' are presented in the Supplementary Material, Tables S5–S9. The production of low-quality biochar from Source 2 starts to reduce at $\psi = 0.8$, and is entirely eliminated at $\psi = 0.4$ and 0.2 (Fig. 7). On the other hand, biochar supply at Sink 1 starts to decrease at $\psi = 0.8$ and is completely removed at $\psi = 0.4$ and 0.2 (Fig. 8). The result is interesting since network complexity is minimized with the exclusion of Source 2 and Sink 1 at $\psi = 0.4$ and 0.2. Comparison of Scenarios 1 and 2 at $\psi = 1$ is clearly depicted in Fig. 9. The same trend is also observed for other values of ψ (Appendix, Figs. C.1 and C.2). It is evident that the CO_2 sequestration achieved in Scenario 2 is substantially higher than what is attained in Scenario 1. This finding signifies the necessity of properly assessing the carbon sequestration potential of biochar to realize its maximum sustainable potential to mitigate climate change.

3.3. Sensitivity analysis with respect to biochar market price

The sensitivity of profit and carbon sequestration to biochar price at $\psi = 1$ in Scenario 1 is given in Fig. 10. The same trend is also observed for Scenario 2. It can be seen that the maximum carbon sequestration achievable by the system is 856,748 t for all the biochar prices used in the case study. The effect of biochar pricing is more significant in profit than in CO_2 sequestration. For instance, the values of CO_2 sequestration remain the same when biochar price is equal to US\$10/t, US\$20/t, and US\$30/t. It can be observed that the points in each Pareto front draw closer as the biochar price increases. While the inclination is to choose among the data points that lie in the Pareto front when biochar price is equal to \$100/t, it is also imperative to consider the effect of biochar pricing to the farmers who are the ultimate consumers of biochars.

4. Conclusion

In this work, a bi-objective MILP model is developed for the synthesis of biochar-based CMNs. The model takes into account both economic (profit) and environmental (carbon sequestration) aspects. The model also incorporates a risk aversion parameter to calibrate the decision-maker's tolerance to the extent of soil contamination risk. These features are decisive factors that can guide decision-making during the large-scale implementation of biochar-based CMNs. The multi-period source-sink model formulation allows the biochar streams to be blended and allocated to ensure that the contaminant limits of the receiving soils are not exceeded. Unlike previous formulations, a unique sequestration factor can be specified for each source-sink pair to account for complex interactions between the biochars and soils in the CMN. This indicates that proper evaluation of the carbon sequestration potential of biochar is indeed critical to reach its full sustainable potential to mitigate climate change. This model can be extended in the future to account for the incompatibilities of biochar sources

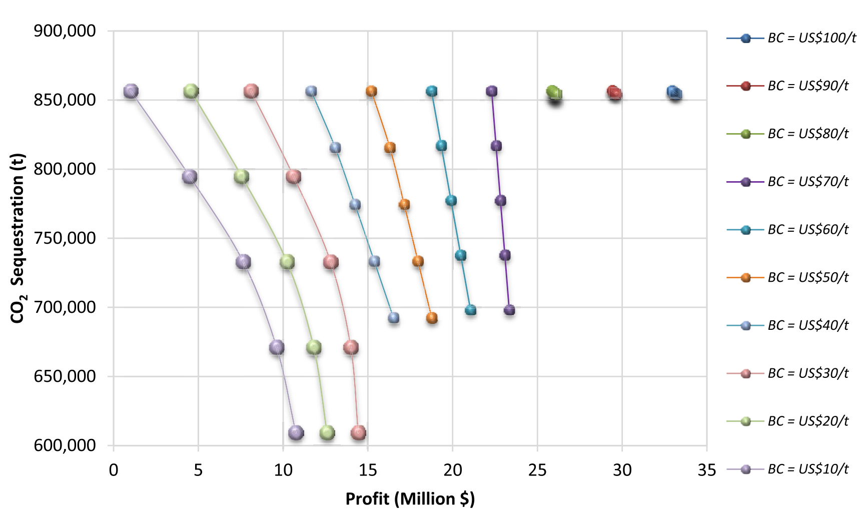

Fig. 10. Sensitivity of profit and carbon sequestration to biochar price at $\psi = 1$ in Scenario 1.

and sinks, as well as process variables in the sources to allow for control of biochar characteristics. Additional parameters, variables and constraints can be introduced to account for such interactions.

Acknowledgment

The financial support of the Philippine Department of Science and Technology (DOST) via the Engineering Research and Development for Technology (ERDT) program is gratefully acknowledged.

Appendix A. MILP model for biochar-based CMN

A.1. Nomenclature

Sets

I	Biochar sources
J	Biochar sinks
K	Biochar contaminants
P	Time periods

Indexes

i	Biochar source index ($i = 1, 2, 3 \ldots M$)
j	Biochar sink index ($j = 1, 2, 3 \ldots N$)
k	Biochar contamination index ($k = 1, 2, 3 \ldots Q$)
p	Time period index ($p = 1, 2, 3 \ldots T$)

Parameters

A_{ij}	Sequestration factor of biochar (t CO_2/t)
B_{ij}	Transportation emissions factor for biochar from source i to sink j (t CO_2/t)
Cf_i	Dimensionless conversion factor of bio-oil from source i
D_{jp}	Annual biochar application dosage at sink j in period p (t/y)
d_{ij}	Distance between source i and sink j (km)
L_j	Limiting biochar storage capacity of sink j (t)
Q_{ikp}	Concentration of contaminant k in biochar produced by source i in period p (ppm or g/t)
Q^*_{jk}	Concentration limit of contaminant k in biochar used in sink j (ppm or g/t)
S^L_{ip}	Lower limit of biochar production rate of source i in period p (t/y)
S^U_{ip}	Upper limit of biochar production rate of source i in period p (t/y)
T	Duration of planning horizon (y)
ψ	Risk aversion parameter

Variables

b_i	Binary variable for source i
b_{ij}	Binary variable for biochar allocated from source i to sink j
S_{ip}	Biochar production rate of source i in period p (t/y)
x_{ijp}	Allocation of biochar for sink j coming form source i during the period p (t/y)

A.2. Optimization model (Tan, 2016)

$$\text{maximize } \Sigma_i \Sigma_j \Sigma_p A_i x_{ijp} - \Sigma_i \Sigma_j \Sigma_p B_{ij} x_{ijp} \tag{A.1}$$

subject to:

$$\Sigma_j x_{ijp} = s_{ip} \quad \forall i, p \tag{A.2}$$

$$\Sigma_i x_{ijp} \le D_{jp} \quad \forall j, p \tag{A.3}$$

$$\Sigma_i \Sigma_p x_{ijp} \le L_j \quad \forall j \tag{A.4}$$

$$\Sigma_i x_{ijp} Q_{ikp} \le D_{jp} Q^*_{jk} \psi \quad \forall j, k, p \tag{A.5}$$

$$b_i s^L_{ip} \le s_{ip} \le b_i s^U_{ip} \quad \forall i \tag{A.6}$$

$$b_i \in \{0, 1\} \quad \forall i \tag{A.7}$$

$$0 \le x_{ijp} \le b_{ij} s^U_{ip} \quad \forall i, j, p \tag{A.8}$$

$$b_{ij} \in \{0, 1\} \quad \forall i, j \tag{A.9}$$

The objective of the model is to maximize the net CO_2 sequestration denoted by Eq. (A.1). Equations (A.2–A.5) depict the biochar balances at the sources and sinks. The limits set for the variables are given by Eqs. (A.6–A.9).

Appendix B. The ε-constraint method (Haimes and Hall, 1974)

Given the following multi-objective optimization problem:

$$\begin{aligned} &\max\ (f_1(x),\ f_2(x) \ldots f_n(x)) \\ &\text{s.t.} \\ &\quad x \in T, \end{aligned}$$

where x represents a vector of decision variables, $f_1(x), f_2(x), \ldots f_n(x)$ represents the n objective functions and T is the feasible decision space.

The ε-constraint approach optimizes one of the objective functions while incorporating other objective functions as additional constraints to the optimization model.

$$\begin{aligned} &\max \quad f_1(x) \\ &\text{s.t.} \quad f_j(x) \ge \varepsilon_j, j = 2, 3 \ldots n \\ &\qquad\ x \in T. \end{aligned}$$

The efficient solutions of the problem are attained via parametric variation in ε_j.

Appendix C. Comparison of Scenarios 1 and 2

Appendix C.1

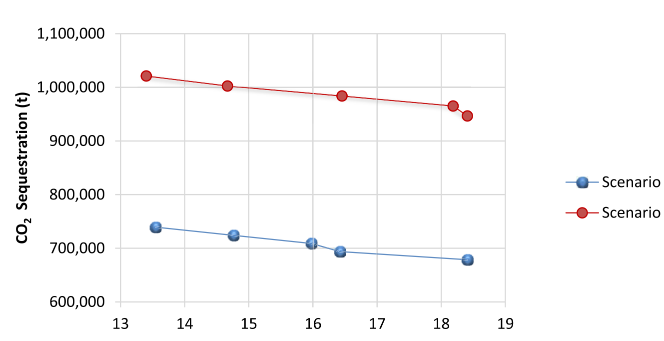

Fig. C.1. Comparison of Pareto frontiers of Scenarios 1 and 2 at $\psi = 0.8$.

Appendix C.2

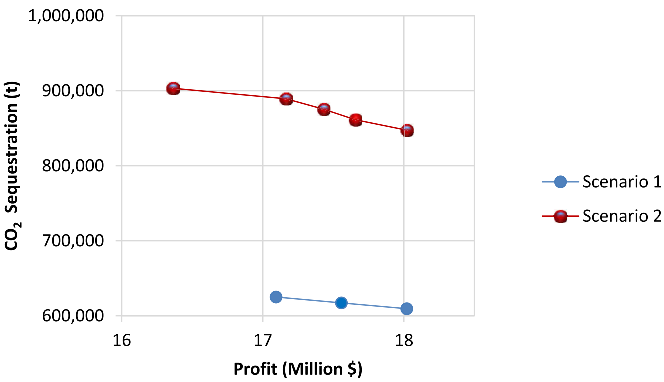

Fig. C.2. Comparison of Pareto frontiers of Scenarios 1 and 2 at $\psi = 0.6$.

Appendix D. Supplementary data

Supplementary data related to this article can be found at https://doi.org/10.1016/j.jclepro.2018.04.023.

References

Abdul Qados, A.M.S., 2011. Effect of salt stress on plant growth and metabolism of bean plant Vicia faba (L.). Journal of the Saudi Society of Agricultural Sciences 10, 7–15.

Ahmed, M.B., Zhou, J.L., Ngo, H.H., Guo, W., 2016. Insight into biochar properties and its cost analysis. Biomass Bioenergy 84, 76–86.

Belmonte, B.A., Benjamin, M.F.D., Tan, R.R., 2017. Biochar systems in the water-energy-food nexus: the emerging role of process systems engineering. Current Opinion in Chemical Engineering 18, 32–37.

Bong, C.P.C., Lim, L.Y., Ho, W.S., Lim, J.S., Klemeš, J.J., Towprayoon, S., 2017. A review on the global warming potential of cleaner composting and mitigation strategies. J. Clean. Prod. 146, 149–157.

Crombie, K., Mašek, O., 2015. Pyrolysis biochar systems, balance between bioenergy and carbon sequestration. GCB Bioenergy 7, 349–361.

Crombie, K., Mašek, O., Sohi, S.P., Brownsort, P., Cross, A., 2013. The effect of pyrolysis conditions on biochar stability as determined by three methods. GCB Bioenergy 5, 122–131.

Foo, D.C.Y., Tan, R.R., Loong, H., Kamal, M., Aziz, A., 2013. Robust models for the synthesis of flexible palm oil-based regional bioenergy supply chain. Energy 55, 68–73.

Fornes, F., Belda, R.M., Lidón, A., 2015. Analysis of two biochars and one hydrochar from different feedstock: focus set on environmental, nutritional and horticultural considerations. J. Clean. Prod. 86, 40–48.

Galinato, S.P., Yoder, J.K., Granatstein, D., 2011. The economic value of biochar in crop production and carbon sequestration. Energy Pol. 39, 6344–6350.

Haimes, Y.Y., Hall, W.A., 1974. Multiobjectives in water resource systems analysis: the surrogate worth trade off method. Water Resour. Res. 10, 615–624.

He, Y., Zhou, X., Jiang, L., Li, M., Du, Z., Zhou, G., Shao, J., Wang, X., Xu, Z., Hosseini Bai, S., Wallace, H., Xu, C., 2017. Effects of biochar application on soil greenhouse gas fluxes: a meta-analysis. GCB Bioenergy 9, 743–755.

Jirka, S., Tomlinson, T., 2014. State of the biochar industry 2013-a survey of commercial activity in the biochar field. International Biochar Initiative 1–61. www.biochar-international.org/sites/default/files/StateoftheBiocharIndustry_2013_4pager_final.pdf. (Accessed 13 May 2017).

Kahn, B., 2017. We just breached the 410 parts per million threshold. www.climatecentral.org/news/we-just-breached-the-410-parts-per-million-threshold-21372. (Accessed 12 May 2017).

Kasivisvanathan, H., Ng, R.T.L., Tay, D.H.S., Ng, D.K.S., 2012. Fuzzy optimisation for retrofitting a palm oil mill into a sustainable palm oil-based integrated biorefinery. Chem. Eng. J. 200–202, 694–709.

Kulyk, N., 2012. Cost-benefit Analysis of the Biochar Application in the U. S. Cereal Crop Cultivation. School of Public Policy Capstones, p. 12. scholarworks.umass.edu/cppa_capstones/12/. (Accessed 17 May 2017).

Lee, C.T., Hashim, H., Ho, C.S., Fan, Y.Van, 2017. Sustaining the low-carbon emission development in Asia and beyond: sustainable energy , water , transportation and low-carbon emission technology. J. Clean. Prod. 146, 1–13.

Major, J., 2010. Guidelines on practical aspects of biochar application to field soil in various soil management systems. International Biochar Initiative 1–23. www.biochar-international.org/sites/default/files/IBI%20Biochar%20Application%20Guidelines_web.pdf. (Accessed 15 May 2017).

McGlashan, N., Shah, N., Caldecott, B., Workman, M., 2012. High-level techno-economic assessment of negative emissions technologies. Process Saf. Environ. Protect. 90, 501–510.

McLaren, D., 2012. A comparative global assessment of potential negative emissions technologies. Process Saf. Environ. Protect. 90, 489–500.

Muñoz, E., Curaqueo, G., Cea, M., Vera, L., Navia, R., 2017. Environmental hotspots in the life cycle of a biochar-soil system. J. Clean. Prod. 158, 1–7.

Regional Profile: Central Luzon. countrystat.psa.gov.ph/?cont=16&r=3 (accessed 12 September 2017).

Sheng, Y., Zhan, Y., Zhu, L., 2016. Reduced carbon sequestration potential of biochar in acidic soil. Sci. Total Environ. 572, 129–137.

Tan, R.R., 2016. A multi-period source-sink mixed integer linear programming model for biochar-based carbon sequestration systems. Sustainable Production and Consumption 8, 57–63.

Tan, Z., Lin, C.S.K., Ji, X., Rainey, T.J., 2017. Returning biochar to fields: a review. Appl. Soil Ecol. 116, 1–11.

Vereš, J., Kolonicný, J., Ochodek, T., 2014. Biochar status under international law and regulatory issues for the practical application. Chemical Engineering Transactions 37, 799–804.

Windeatt, J.H., Ross, A.B., Williams, P.T., Forster, P.M., Nahil, M.A., Singh, S., 2014. Characteristics of biochars from crop residues: potential for carbon sequestration and soil amendment. J. Environ. Manag. 146, 189–197.

Woolf, D., Amonette, J.E., Street-Perrott, F.A., Lehmann, J., Joseph, S., 2010. Sustainable biochar to mitigate global climate change. Nat. Commun. 1, 56. https://doi.org/10.1038/ncomms1053.

Wrobel-Tobiszewska, A., Boersma, M., Sargison, J., Adams, P., Jarick, S., 2015. An economic analysis of biochar production using residues from Eucalypt plantations. Biomass Bioenergy 81, 177–182.

Xu, Y., Ramanathan, V., 2017. Well below 2 °C: mitigation strategies for avoiding dangerous to catastrophic climate changes. Proc. Natl. Acad. Sci. Unit. States Am. 114, 10315–10323.